

Read Pointer Meters in complex environments based on a Human-like Alignment and Recognition Algorithm

Yan Shu, Shaohui Liu, Honglei Xu and Feng Jiang
Harbin Institute of Technology

Abstract Recently, developing an automatic reading system for analog measuring instruments has gained increased attention, as it enables the collection of numerous state of equipment. Nonetheless, two major obstacles still obstruct its deployment to real-world applications. The first issue is that they rarely take the entire pipeline's speed into account. The second is that they are incapable of dealing with some low-quality images (i.e., meter breakage, blur, and uneven scale). In this paper, we propose a human-like alignment and recognition algorithm to overcome these problems. More specifically, a Spatial Transformed Module(STM) is proposed to obtain the front view of images in a self-autonomous way based on an improved Spatial Transformer Networks(STN). Meanwhile, a Value Acquisition Module(VAM) is proposed to infer accurate meter values by an end-to-end trained framework. In contrast to previous research, our model aligns and recognizes meters totally implemented by learnable processing, which mimics human's behaviours and thus achieves higher performances. Extensive results verify the good robustness of the proposed model in terms of the accuracy and efficiency. The code and the datasets will be available in <https://github.com/shuyansy/A-detection-and-recognition-pipeline-of-complex-meters-in-wild>.

Keywords Analog measuring instruments, Pointer meters reading, Spatial Transformed Module, Value Acquisition Module

1 Introduction

In the complex industrial environment, there are harsh environments such as radiation, toxic, high temperature, etc., it is necessary to inspect the production condition with the help of instruments to ensure safety[1]. Traditionally acquired data is typically read artificially by humans, who are capable of deriving precise readings from complex meters in a variety of shapes, forms, and styles, despite never having seen the meter in question. However, the manual method is always more labor intensive and time consuming. So it is of great practical significance to rely on inspection robots and computer vision technology[2, 3, 4, 5] for automatic meter reading.

Substation meters are now classified as digital and pointers. While reading digital meters can be considered an OCR task and is relatively simple to accomplish using text spotting techniques[6, 7, 8, 9], reading pointer meters presents a different and more difficult

problem: there are major visual changes between meter faces, the camera viewpoint has a significant effect on their depicted shape and numbering location, and the existence of shadows, meter breakage, and specular reflections adds to the pointer hands' perplexity. While this issue has been around for a long time, few previous solutions have been capable of reliably obtaining readings from meters, except in extremely limited circumstances. Additionally, it is difficult for researchers to work on this project due to the lack of reliable training and evaluation standards.

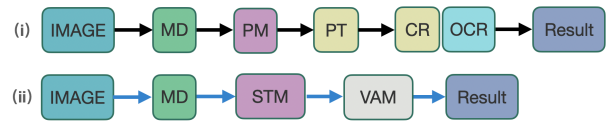


Fig.1. Overview of previous pointer meter reading pipeline (i) compared to ours (ii). The “MD”, “PM”, “PT”, and “CR” mean Meter Detection, Points Matching, Perspective Transform, and Component Retrieval, respectively. “STM” and “VAM” mean Spatial Transformed Module and Value Acquisition Module we proposed.

Existing automatic meter reading systems[10, 11,

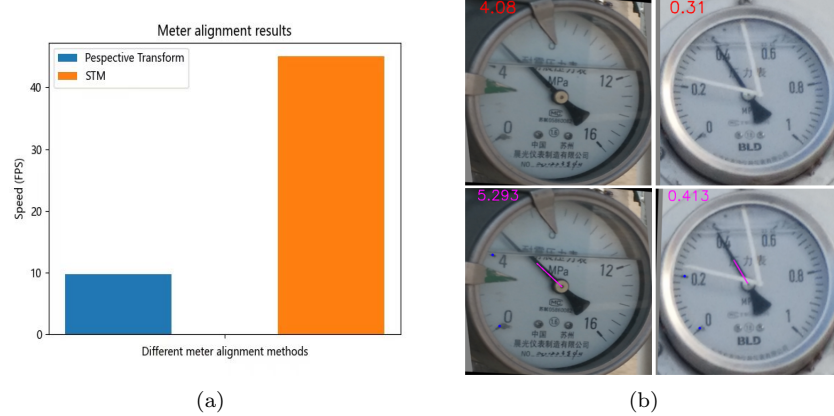


Fig.2. (a) shows the efficiency of our STM for meter alignment, which is 5 times faster than the conventional perspective transform method. (b) shows our VAM (bottom line) can read more accurate values in some low-quality images than prior methods (top line).

12, 13], according to relevant literature, include the following pipelines: To begin, the meter’s pure area is detected using conventional neural network-based detection algorithms or image processing techniques; then the captured target is aligned to a front view by perspective transform method. Lastly, meter values can be obtained by meter component (the pointer and the scale) retrieval and meter number recognition. However, most of these methods suffer from two main problems. First, the alignment process is typically time-consuming due to its intricate point-matching steps, which hinders the overall efficiency of the system. Second, their reading model is not robust; it consists of isolated and independent modules for meter component retrieval and number recognition, which are unaware of their interdependence, resulting in poor accuracy. Therefore, “how to design an algorithm for efficient alignment and robust recognition of pointer meters” remains largely unsolved.

To address these issues, we propose a novel human-like alignment and recognition algorithm, which simplifies the meter reading pipeline as shown in Fig 1. To be more precise, we propose a novel Spatial Transformed Module (STM) for alignment via implicitly learning homography transformation, which is heavily inspired by

the Spatial Transformer Networks (STN)[14]. STM is more efficient to align meter than previous morphological conversion methods by discarding point-matching process. Additionally, a Value Acquisition Module (VAM) is established in a unified framework of meter component retrieval and meter number recognition, simulating the structure of an end-to-end text spotter. By excavating the relationship between meter components and meter number, VAM can learn a richer representation and thus can read precise meter values from low-quality images. As shown in Fig 2, on the MC1260 dataset we proposed, the FPS of STM is 50 FPS which is 5 times faster than the conventional alignment method. Meanwhile, VAM can handle some difficult data such as meter breakage, blur and uneven scale.

In this paper, we make the following contributions:

- (i) We design a unified framework involving detection, alignment and recognition stages. The detection can simply be an off-the-shelf object detection model. The alignment stage involves a deep neural network which introduces an improved STN to regress homography transformation parameters implicitly. At the recognition stage, we are the first to establish an end-to-end architecture to tightly couple meter component

retrieval and meter number recognition, boosting both the accuracy and efficiency of the pointer meter reading.

(ii) We propose a new benchmark dataset called Meter_Challenge (MC1296) which contains 1296 images captured in scene by automatic robots. MC1296 is organized in a tree structure, containing images, annotations and evaluation metrics for different tasks (meter detection, meter alignment, and meter recognition) from top to bottom.

(iii) Extensive experiments verify the effectiveness and robustness of the method we propose.

The rest of this paper is organized as follows. The related background knowledge is provided in Section 2, including the previous pointer meter reading pipelines, the Spatial Transformer Networks (STN) and the end-to-end text spotting methods highly related to our works. Section 3 introduces the implementation process of the proposed method. In Section 4, the proposed method is verified by extensive simulation experiments and ablation studies. The conclusions of this paper are summarized in Section 5.

2 Related Works

We commence this section by reviewing major pointer meter reading frameworks. Additionally, we discuss the research on STN and end-to-end text spotting methods which are highly relevant to our works.

2.1 Pointer meter reading frameworks

Numerous advances[10, 11, 12, 13, 15, 16, 17, 18] have been made in the reading of pointer meters over the last few years. The existing frameworks are generally divided into three stages: meter detection, meter alignment, and meter recognition. Traditional algorithms[18] such as template matching and the table lookup method are used in meter detection. To

address this issue with complex backgrounds, some object detection methods such as Faster RCNN[13] have been introduced. In order to calibrate the camera angle to get a front view image, perspective transform techniques[13, 11] are applied by calculating transformation matrix determined by points matching. Image processing methods[19] also propose using the image subtraction method or the Hough Transform algorithm to extract the pointer for meter recognition. Additionally, machine learning and deep learning are used to improve reading accuracy. While He et al.[16] improve the Mask RCNN[20] method for pointer segmentation. Following that, final values can be determined by calculating the pointer angle and meter number output. The majority of the aforementioned approaches are able to read pointer meters, but few of them can balance accuracy and speed due to complex post-processing in meter alignment[13] or inadequate visual representations in meter recognition.

2.2 Spatial Transformer Networks(STN)

In contrast to the conventional perspective transform method, which explicitly calculates the transformation matrix. STN[14] introduces a novel learnable module that enables spatial manipulation of data within the network. STN is advantageous for a wide variety of computer vision tasks due to its efficiency and flexibility. ASTER[21] consists of a rectification network and a recognition network that can deal with text that is distorted or has an irregular layout. Lee et al.[22] propose Image-and-Spatial Transformer Networks (ISTNs) for downstream image registration optimization. Additionally, Yang et al.[23] introduce a clock alignment architecture based on STN, which motivates us to develop a more efficient meter alignment module.

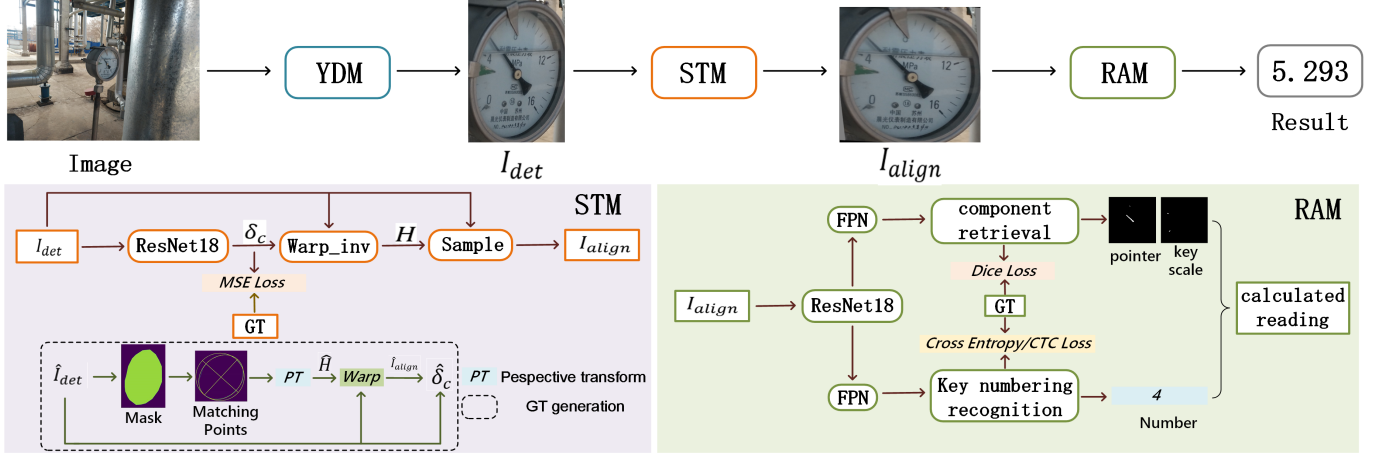


Fig.3. The proposed framework of the pointer meter recognition. YDM can detect meter targets and crop meter regions into STM, where aligned views can be obtained. VAM can output meter values accurately and efficiently.

2.3 End-to-end text spotters

To spot texts in images, a straight two-stage idea is proposed to cascade existing detector and recognizer sequentially. However, due to the lack of complementarity between detector and recognizer, they suffer from low efficiency and accuracy. To mitigate this problem, an end-to-end trainable Neural Network for text spotting is attempted, with state-of-the-art performances achieved. Li et al. [24] first builds an unified end-to-end work that simultaneously localizes and recognizes text with a single forward pass, with positive results achieved in horizontal text spotting task. Benefiting from convolution sharing strategy, FOTS [25] and EAA [26] pool multi-oriented text regions from feature map by designing ROI Rotate and Text-Alignment layer, respectively. Unfortunately, few of researchers take end-to-end text spotters into their pointer meter recognition frameworks.

Our work is structured similarly to existing frameworks for pointer meter reading. To increase the applicability of previous work, we replace the traditional perspective transform method by an improved STN and then create an end-to-end meter recognition module for meter component retrieval and meter number recogni-

tion.

3 Methods

The purpose of this paper is to design an algorithm for efficient alignment and robust recognition of pointer meters. To achieve this goal, we establish a unified framework, which is shown in Fig 3. Our proposed architecture accepts an image as input and then performs detection, alignment, and recognition sequentially. It is noteworthy that our STM (see Sec.3.2) can directly transform the detected meter into an aligned view without any post-processing steps. Meanwhile, the VAM (see Sec.3.3) we proposed can learn rich visual representation by excavating the relationship between component retrieval and number recognition.

3.1 Meter Detection

Cropping meter regions prior to recognition is necessary to eliminate background interference. To accomplish this, some traditional image processing techniques such as Hough Circle Detection and Template Matching are used, both of which have shortcomings in some low-quality images. At the moment, object detection networks are used to detect and crop the meter, as follows.

$$I_{det} = \Phi_{det}(I; \Theta_{det}) \in \mathbb{R}^{3 \times h \times w} \quad (1)$$

where I is the given unlabeled image, while Φ_{dec} and Θ_{dec} represent detecting function and learnable parameters, respectively.

The detector actually can be done using any off-the-shelf object detector. However, to reduce the efficiency cost and handle small meter targets, we propose a YOLO-based Detection Module (YDM) based on YOLO-v5[27], which has achieved promising performance in many tasks. To achieve a better performance in our tasks where data is scarce and target is small, we apply multi-scale training strategy and artificially augment the images by copy-pasting some small objects. The performance of YDM can be seen in Sec. 4.

3.2 Meter Alignment

Motivation. The detected pure meter image could be directly passed to a module for reading recognition. This is typically not ideal for two reasons: first, due to the limitations of the localisation module; and second, even when the meter is properly localised, it can be hard to read at times due to the viewpoint’s interference. Previous methods apply directly perspective transform to calibrate the camera angle to get a front view image as shown in follows:

$$(x, y, w') = (u, v, w) \cdot T = (u, v, w) \cdot \begin{bmatrix} a_{11} & a_{12} & a_{13} \\ a_{21} & a_{22} & a_{23} \\ a_{31} & a_{32} & a_{33} \end{bmatrix} \quad (2)$$

$$(X, Y) = \left(\frac{x}{w'}, \frac{y}{w'} \right) \quad (3)$$

$$(U, V) = \left(\frac{u}{w'}, \frac{v}{w'} \right)$$

where (U, V) represents the coordinate of a point in the original image, (X, Y) is the coordinate of the corresponding point in the transformed image, (u, v, w) and (x, y, w') are the homogenous space representation

of (U, V) and (X, Y) , respectively. By matching four feature points between two images, transform matrix T is determined. Their methods, however, suffer primarily from complex points matching algorithms, which are time-consuming and not very robust. This drives us to design a more efficient and stronger module for meter alignment.

Revisiting vanilla STN. Different from Perspective Transform which calculates transformation matrix by points matching, STN can transform the detected meter to a fronto-parallel view by learned homography transformation parameters. Specifically, given the output I_{det} of YDM, STN establishes mapping ϕ_{stn} by predicting homography transformation H with 8 degree of freedoms, and ϕ_{sam} represents Differentiable Image Sampling(DIS) operation to obtain the canonical view of I_{det} by bilinear interpolation:

$$H = \Phi_{stn}(I_{det}) \in \mathbb{R}^{3 \times 3} \quad (4)$$

$$I_{align} = \Phi_{sam}(I_{det}, H) \in \mathbb{R}^{3 \times h \times w}$$

Therefore, how to predict accurate homography transformation H is a key issue.

Spatial Transformed Module(STM). It is a direct idea to regress H given ground truth \hat{H} in a supervised way. Nonetheless, based on our major findings and rigorous testing, the deep network fails to learn the explicit parameter of H for the following reasons: (i) The training data is limited to the deep CNN’s huge parameters; (ii) H ’s parameters have a large range of values, making the regression difficult to optimise. To circumvent these problems, we model the implicit spatial transformation relationship between images instead of regressing H directly.

Specifically, for a \hat{I}_{det} in training set, we firstly annotate its inner dial region with a binary mask map. Then, for various meter forms, we match four pairs of feature points to determine the real \hat{H} . As for an irreg-

ular ellipse, the endpoints of the major axis and minor axis are utilized as the initial points, while the corresponding points are defined by the intersection of the major axis, the minor axis, and the circumcircle. For a rectangular shape, the \hat{H} can be calculated by mapping the vertices of the rectangle directly to the vertices of the image. Then we can get the aligned image \hat{I}_{align} by perspective transform:

$$\hat{I}_{align} = warp(\hat{I}_{det}, \hat{H}) \quad (5)$$

The vertex coordinate offsets $\hat{\delta}_c$ between \hat{I}_{det} and \hat{I}_{align} can be obtained, which is the training objective of STM implemented by Mean-Squared (MSE) Loss:

$$L_{align} = \sum_i (\delta_{ci} - \hat{\delta}_{ci})^2 \quad (6)$$

Where i is the index of coordinates. Therefore, the algorithm of STM can be adjusted as follows:

$$\begin{aligned} \delta_c &= \Phi_{stm}(I_{det}) \in \mathbb{R}^{4 \times 2} \\ H &= warp_inv(I_{det}, I_{det} + \delta_c) \in \mathbb{R}^{3 \times 3} \end{aligned} \quad (7)$$

$$I_{align} = \Phi_{sam}(I_{det}, H) \in \mathbb{R}^{3 \times h \times w}$$

In our training process, we use ResNet18[28] to extract the feature of I_{det} , and by the propagation of network, accurate H and canonical images can be acquired.

3.3 Meter Recognition

Overall Design. What is the best way to read meters like a human? Key meter elements like the pointer, scales, and number were predicted in previous methods to achieve this goal. However, they tended to create independent modules to handle different component and number, resulting in a suboptimal solution for meter recognition. We propose a unified framework called Value Acquisition Module (VAM) that consists of meter

component retrieval branch and meter number recognition branch to excavate a deep relationship between them. As illustrated in Fig 3, we apply ResNet18 as the backbone and create two separate feature merging modules to form a pair of complementary branches. Specifically, upsampling and pixel-wise addition are used to fuse intermediate layers of ResNet. VAM allows these two diametrically different tasks to benefit from each other by disentangling weight sharing and introducing a mirror symmetry of FPN[29]. Ablation studies are demonstrated in Sec. 4.

Meter component retrieval branch. We retrieve meter component (meter pointer and key scales) using semantic segmentation methods that are heavily inspired by the Mask-RCNN[20]. The branch generates two 1-channel segmentation maps, namely the Pointer Map and the Key Scale Map, by performing two distinct 1×1 convolutional operations on the backbone features. The Pointer Map indicates the location of the meter's pointer, whereas the Key Scale Map indicates its angle. The Pointer Map and Key Scale Map are both trained by minimizing the Dice loss:

$$\begin{aligned} L_{pm} &= 1 - \frac{2 \sum_i P_{pm}(i) G_{pm}(i)}{\sum_i P_{pm}(i)^2 + \sum_i G_{pm}(i)^2} \\ L_{ksm} &= 1 - \frac{2 \sum_i P_{ksm}(i) G_{ksm}(i)}{\sum_i P_{ksm}(i)^2 + \sum_i G_{ksm}(i)^2} \end{aligned} \quad (8)$$

where pm and ksm represent Pointer Map and Key Scale Map, and $P_{(.)}(i)$ refer to the value of i^{th} pixel in the predicted result while $G_{(.)}(i)$ refer to the value of i^{th} pixel in the GT region.

The final loss for the meter component retrieval branch is a weighted combination of the two maps, balanced by $\lambda \in (0, 1)$ as

$$L_{com} = \lambda L_{PointerMap} + (1 - \lambda) L_{KeyScaleMap} \quad (9)$$

In our experiments, we set λ to 0.4, assigning more

importance to Key Scale Map, which is relatively difficult to learn in training process due to its small spatial occupation.

Meter number recognition branch. Previous methods recognize numbers in meters with another system, which poses severe memory waste and low efficiency. In our VAM, meter number recognition branch resembles like the standard text spotters, which is mentioned in Sec.2. To further boost the inference speed, We only detect the key number in the meter, the one closest to the number ‘0’, and then recognize it with the assistance of feature sampling.

The key number detection task is deemed a text classification task, in which one convolution is applied to output dense per-pixel predictions of the key number localization. The key number bounding box can be obtained by the minimum bounding rectangle operation. Meanwhile, to overcome the class imbalance problem, we introduce online hard example mining (OHEM)[30] to better distinguish between number areas and backgrounds, in which the balanced factor is set to 3 in our work. The set of selected positive elements by OHEM in the score map as ω , the loss function for key number detection can be formulated as:

$$\begin{aligned} L_{num_det} &= \frac{1}{\|\Omega\|} \sum_{x \in \Omega} \text{Cross_Entropy}(p_x, p_x^*) \\ &= \frac{1}{\|\Omega\|} \sum_{x \in \Omega} (-p_x^* \log p_x - (1 - p_x^*) \log(1 - p_x)) \end{aligned} \quad (10)$$

where $\|\cdot\|$ means the number of elements in a set, and the p_x and p_x^* are the predicted pixel and the ground truth label, respectively.

The feature sampling layer aims to convert detected feature regions into fixed-size outputs from which a RNN-based sequence recognizer can be established. We introduce RoIRotate in [8] to our work, which can transform the rotated area into a fixed-size region via max-

pooling and bilinear interpolation. Similar to but distinguished from STN, RoIRotate gets affine transformation via an unsupervised way, resulting in a more general operation for extracting features for regions of interest. To improve recognition performance, we use only ground truth key number regions during training rather than predicted number regions.

Given the transformed number feature, we first permute key number features $F \in \mathbb{R}^{C \times H \times W}$ into 2D sequence feature $L \in \mathbb{R}^{C \times W}$ in several sequential convolutions, which has the same configurations as CRNN[31]. Then, for each time step $t = 0, 1, \dots, T + 1$, we feed $l_1, \dots, l_w \in L$ into bi-directional LSTM, with D=256 output channels per direction, which can be formulated as follows:

$$\begin{aligned} h_t' &= f(x_t, h_{t-1}') \\ y_t &= \varphi(h_t') = \text{softmax}(W_0 h_t') \end{aligned} \quad (11)$$

where $f()$ is the recurrence formulation, h_t is the hidden state at time step t , and the W_0 linearly transforms hidden states to the output space of size 12, including 10 Arabic numerals and a token representing “.”, and a special END token. Finally, a CTC layer is applied to align the predicted sequence to label sequence. Following[31], the recognition loss can be formulated as

$$L_{num_reco} = -\frac{1}{N} \sum_{n=1}^N \log p(y_n^* | x) \quad (12)$$

where N is the number of number regions in an input image, and y_n^* is the recognition label.

Training procedure and inference. VAM is a unified module which can be trained end-to-end. the overall loss function can be calculated as follows:

$$L = L_{com} + L_{num_det} + L_{num_reco} \quad (13)$$

In our inference process, binarized score maps for pointer and key scale are firstly obtained by applying

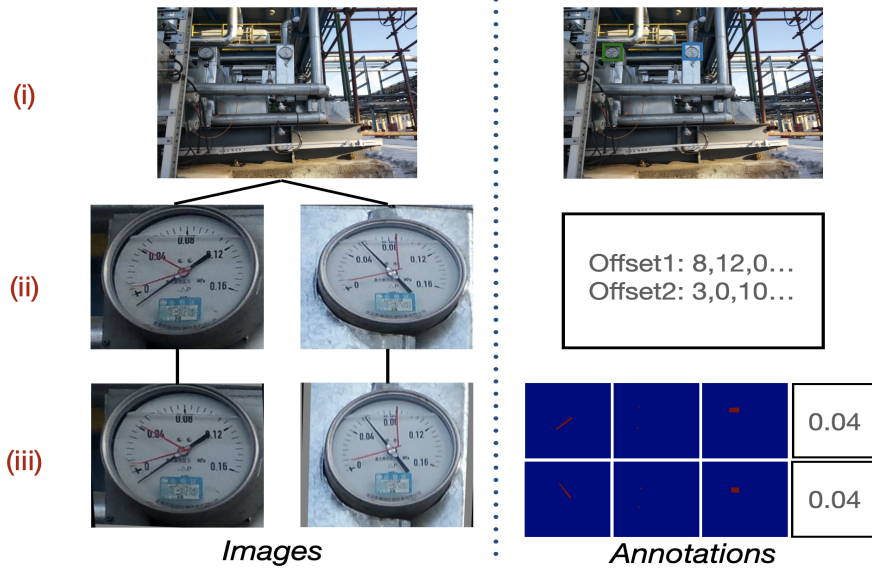


Fig.4. Visualization results of one sample in the data. (i), (ii) and (iii) mean the data for the meter detection, meter alignment, and meter recognition.

threshold algorithm $\lambda = 0.5$. Then, a thinning algorithm is applied to turn the pointer into a straight line segmentation and the Hough line transform is used to obtain the position of the pointer. Meanwhile the key scale centres can be localized by calculating the average pixels position within the closed area. Finally the meter reading is calculated by angle method, which is given by

$$Result = \frac{\alpha_1}{\alpha_2} \times num_rec \quad (14)$$

where α_1 is the angle between the pointer and the zero scale, and α_2 is the angle between the zero scales and the key scale. The num_rec is the output of the meter number recognition branch, then the reading of the meter is completed automatically.

4 Experiments

4.1 Datasets

To our knowledge, there have been no publicly available and appropriate benchmarks for this task. As a result, we created a new dataset called Meter_Challenge

(MC1296), which contains 1296 images of scenes captured by automated robots. To help the model adapt to its natural environment, the dataset includes complex backgrounds, multiple scales, a variety of viewpoint angles, and a variety of meter shapes. To better fit the meter reading task, we organized the dataset into a tree structure, with each level representing a distinct task (meter detection, meter alignment, and meter recognition), complete with associated images, annotations, and evaluation metrics. Fig 4 illustrates some visualization results, while Table 1 contains summary statistics.

Table 1. Statistics of the proposed MC_1260 dataset. "mb", "co", "psn" represent meter bounding box, coordinate offsets, and pointer/scale/number mask and number, respectively.

Dataset_task	Train_size	Test_size	Annotations
M_detection	1036	260	mb
M_alignment	1028	247	co
M_reading	739	185	psn

4.2 Implementation details

In this paper, the system we propose consists of YDM, STM, and VAM. YDM has the similar configurations with [27], so we focus on the implement of STM

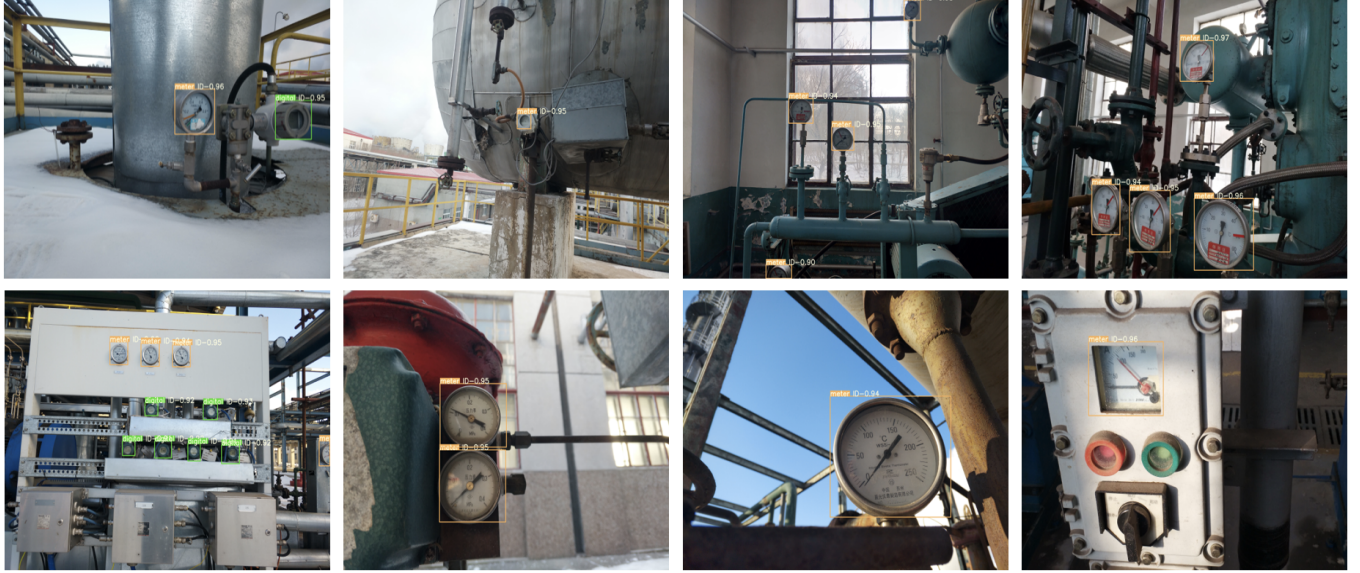


Fig.5. Qualitative results of the meter detection, where yellow bounding box means pointer meter and green bounding box means digital meter. “ID-num” is the detection confidence.

and VAM. Specifically, for both of the module we use ResNet pretrained in ImageNet[32] as backbone, and the image size is 640 and the training batch size is 8. We use Adam to optimizer the two network and set the initial learning rate to 1×10^{-4} with the momentum of 0.9.

Meanwhile, some basic data augmentation techniques are applied, such as the random cropping, random rotation, and the brightness contrast. Our experiment is conducted on one general GPU (GTX-1080), with the environment PyTorch 1.5.0.

4.3 Meter detection results

To disentangle the effects of YDM, we begin by reporting the dataset’s meter detection results. To conform to the object detection literature, we report the average precision (AP) at two different bounding box IoU thresholds, AP50 and AP75. AP50 denotes the average precision for IoU thresholds greater than 0.5, while AP75 denotes the average precision for IoU thresholds greater than 0.75. As shown in the Table 2, the meter detection task is relatively successful. To

demonstrate the advantages of our method, we compare it to a commonly used YOLO algorithm[33] and the method in [13], which demonstrates that our YDM performs better in terms of accuracy and efficiency. The qualitative results are demonstrated in Fig 5, which shows TDM can detect meters with different shapes and sizes.

Table 2. The quantitative results of different methods for meter detection.

Model	AP50(%)	AP75(%)	FPS
Liu.et al[13]	91.3	89.5	4.3
YOLO[33]	90.0	88.2	6.7
Ours	98.6	97.1	12.4

Table 3. The quantitative results of different methods for meter alignment. “rel” is Average Relative Error and “ref” is Average Reference Error.

Method	Rel(%)	Ref(%)	FPS
None	5.91	1.20	-
Perspective transform[13]	1.72	0.23	10
STN[14]	3.40	0.95	44
STM	1.70	0.26	50



Fig.6. Qualitative results of the meter alignment, where the top row is the original images, the middle row and the bottom row are the transformed image generated by STN and STM. Note that STN can not handle images with extreme large camera angles.

4.4 Meter alignment results

To demonstrate the STM’s availability and robustness in the recognition system, we conducted extensive experiments on the validation dataset, comparing it to the traditional perspective transform method and STN. Fig.6 illustrates the qualitative findings. As can be seen, the image can be easily and automatically transformed into a front-viewing image using STM, regardless of the camera angle. However, due to the limited learning capability of pure STN, it is difficult to align the meter in terms of some extremely large camera angles.

Additionally, as shown in Tab 3, we conducted ablation studies to demonstrate its superiority by demonstrating inference speed and influence on meter recognition task. Take note that the average relative error and the average reference error are the evaluation met-

rics used to represent the meter recognition error rate, which will be discussed in detail in Sec 4.5. It can be seen that STM contributes to reduce the recognition error rate as it allows meters to be read from various angles and sizes. Our STM also achieves competitive accuracy to perspective transform while increasing inference speed, indicating that STM achieves a more favorable trade-off between accuracy and efficiency.

4.5 Meter recognition results

To demonstrate our method’s recognition performance, we incrementally compare it to other methods. To minimize inter-person variability in readings, the readings obtained by human vision are the average of the results of twenty expert workers. Meanwhile, to make the comparison more fair, we follow similar evaluation metrics as [16]. Specifically, we choose the average relative error $\hat{\Theta}$ and the average reference error $\hat{\Gamma}$



Fig.7. Some visualization results produced by our method. The red line is the predicted pointer line, the blue points are the key scale areas, and the meter reading results are shown in the left top.

as evaluation indicators, as shown in follow

$$\hat{\Theta} = \frac{\sum_{i=1}^n \frac{|p_i - g_i|}{g_i}}{n} \times 100\% \quad (15)$$

$$\hat{\Gamma} = \frac{\sum_{i=1}^n \frac{|p_i - g_i|}{R}}{n} \times 100\%$$

Where p_i is the predicted meter value, g_i is the ground truth value. R represents the meter's range, and n represents the total number of experimental data. As shown in Tab 4, our method outperforms previous methods in terms of average relative error and achieves competitive results with [13] in average reference error, indicating that our algorithm has strong capacity in reading recognition. Additionally, our method can perform inference at a rate of approximately 25 frames per second, demonstrating that it is practical for real-world applications. We show some visualization results in Fig 7, demonstrating our method's high adaptability to a complex environment with variable illumination, scale, and image tilt.

Table 4. The quantitative results of different methods for meter reading recognition. “Rel” is Average Relative Error and “Ref” is Average Reference Error.

Method	Avenue	Rel(%)	Ref(%)
Zheng et al.[11]	Measurement(2016)	10.32	0.91
He et al.[16]	ICIST(2019)	1.85	0.30
Liu et al.[13]	Measurement(2020)	1.77	0.24
Ours	-	1.70	0.26

To disentangle the effects of the unified framework VAM, we conduct ablation studies to investigate the relationships between the meter component retrieval and meter numbering recognition branches. We begin by reporting the full model's end-to-end results on the Tab 5. Notably, we evaluate pointer/key scale detection and key number recognition using the AP50 and number-level accuracy recognition metrics, respectively. It can be demonstrated that by optimizing all loss functions simultaneously, our model achieves a reasonable level of success in detection and recognition tasks. Additionally, we construct a two-stage model in which the

meter component retrieval and meter number recognition branches are trained independently. The meter component retrieval network is built by removing the meter number recognition branch, and similarly, the meter number recognition network is built by removing the meter component retrieval branch from the original network. Our proposed VAM outperforms the two-stage method by a significant margin in both the meter component retrieval and meter number recognition tasks. The results indicate that our joint training strategy accelerated the convergence of model parameters.

Table 5. The ablation studies on VAM. “MCRB” and “MNRB” represent we only train the meter component retrieval branch or meter number recognition branch.

Method	pointer_det(%)	key scale_det(%)	key num-ber_reco(%)
VAM	95.6	93.2	88.7
MCRB	93.1	90.5	-
MNRB	-	-	87.2

5 Conclusion

We propose a novel method for accurate and efficient pointer meter reading, which is implemented by the equipment of YDM, STM, and VAM. Specifically, STM can obtain the front view of images autonomously with the improved STN, and VAM can recognize meters accurately with the unified frameworks with the combination of meter component retrieval branch and meter number recognition branch. Experiments on the challenging datasets we proposed demonstrate that the proposed method has a strong capacity for pointer meter reading. Currently, the algorithm has been successfully applied to robots performing substation inspections. Future work will concentrate on model acceleration in order to develop a more efficient framework for video meter reading.

References

- [1] Tsai M C, Ko P J. On-line condition monitoring of servo motor drive systems by hht in industry 4.0. *Journal of the Chinese Institute of Engineers*, 2017, 40(7):572–584.
- [2] Gao J W, Xie H T, Zuo L, Zhang C H. A robust pointer meter reading recognition method for substation inspection robot. In *2017 International Conference on Robotics and Automation Sciences (ICRAS)*, 2017, pp. 43–47.
- [3] Guo R, Han L, Sun Y, Wang M. A mobile robot for inspection of substation equipments. In *2010 1st International Conference on Applied Robotics for the Power Industry*, 2010, pp. 1–5.
- [4] Park J Y, Lee J K, Cho B H, Oh K Y. An inspection robot for live-line suspension insulator strings in 345-kv power lines. *IEEE Transactions on power delivery*, 2012, 27(2):632–639.
- [5] Lu S, Zhang Y, Su J. Mobile robot for power substation inspection: A survey. *IEEE/CAA Journal of Automatica Sinica*, 2017, 4(4):830–847.
- [6] Qin S, Bissacco A, Raptis M, Fujii Y, Xiao Y. Towards unconstrained end-to-end text spotting. In *Proceedings of the IEEE/CVF International Conference on Computer Vision (ICCV)*, October 2019.
- [7] Liao M, Lyu P, He M, Yao C, Wu W, Bai X. Mask textspotter: An end-to-end trainable neural network for spotting text with arbitrary shapes. *IEEE Transactions on Pattern Analysis and Machine Intelligence*, 2021, 43:532–548.
- [8] Liu X, Liang D, Yan S, Chen D, Qiao Y, Yan J. Fots: Fast oriented text spotting with a unified network. In *Computer Vision and Pattern Recognition*, 2018.
- [9] Liu Y, Chen H, Shen C, He T, Jin L, Wang L. Abcnet: Real-time scene text spotting with adaptive bezier-curve network. *arXiv: Computer Vision and Pattern Recognition*, 2020.
- [10] Cai W, Ma B, Zhang L, Han Y. A pointer meter recognition method based on virtual sample generation technology. *Measurement*, 2020, 163:107962.
- [11] Zheng C, Wang S, Zhang Y, Zhang P, Zhao Y. A robust and automatic recognition system of analog instruments in power system by using computer vision. *Measurement*, 2016, 92:413–420.
- [12] Hou L, Qu H. Automatic recognition system of pointer meters based on lightweight cnn and wsns with on-sensor image processing. *Measurement*, 2021, 183:109819.
- [13] Liu Y, Liu J, Ke Y. A detection and recognition system of pointer meters in substations based on computer vision. *Measurement*, 2020, 152:107333.
- [14] Jaderberg M, Simonyan K, Zisserman A et al. Spatial transformer networks. *Advances in neural information processing systems*, 2015, 28.

- [15] Zhang X, Dang X, Lv Q, Liu S. A pointer meter recognition algorithm based on deep learning. In *2020 3rd International Conference on Advanced Electronic Materials, Computers and Software Engineering (AEM-CSE)*, 2020, pp. 283–287.
- [16] He P, Zuo L, Zhang C, Zhang Z. A value recognition algorithm for pointer meter based on improved mask-rnn. In *2019 9th International Conference on Information Science and Technology (ICIST)*, 2019, pp. 108–113.
- [17] Gao J W, Xie H T, Zuo L, Zhang C H. A robust pointer meter reading recognition method for substation inspection robot. In *2017 International Conference on Robotics and Automation Sciences (ICRAS)*, 2017, pp. 43–47.
- [18] Mo W, Pei L, Huang Q, Zhang Y, Fu W, Zhao Y. Development of automatic verification system for high precision pointer instrument based on template. *Electrical Measurement and Instrumentation*, 2017, 54(12):100–105.
- [19] Shi J, Zhang D, He J, Kang C, Yao J, Ma X. Design of remote meter reading method for pointer type chemical instruments. *Process Automation Instrumentation*, 2014, 35(5):77–79.
- [20] He K, Gkioxari G, Dollár P, Girshick R. Mask r-cnn. In *Proceedings of the IEEE international conference on computer vision*, 2017, pp. 2961–2969.
- [21] Shi B, Yang M, Wang X, Lyu P, Yao C, Bai X. Aster: An attentional scene text recognizer with flexible rectification. *IEEE transactions on pattern analysis and machine intelligence*, 2018, 41(9):2035–2048.
- [22] Lee M C, Oktay O, Schuh A, Schaap M, Glocker B. Image-and-spatial transformer networks for structure-guided image registration. In *International Conference on Medical Image Computing and Computer-Assisted Intervention*, 2019, pp. 337–345.
- [23] Yang C, Xie W, Zisserman A. It’s about time: Analog clock reading in the wild. *arXiv preprint arXiv:2111.09162*, 2021.
- [24] Li H, Wang P, Shen C. Towards end-to-end text spotting with convolutional recurrent neural networks. In *2017 IEEE International Conference on Computer Vision (ICCV)*, 2017, pp. 5248–5256.
- [25] Liu X, Liang D, Yan S, Chen D, Qiao Y, Yan J. Fots: Fast oriented text spotting with a unified network. In *2018 IEEE/CVF Conference on Computer Vision and Pattern Recognition*, 2018, pp. 5676–5685.
- [26] He T, Tian Z, Huang W, Shen C, Qiao Y, Sun C. An end-to-end textspotter with explicit alignment and attention. In *2018 IEEE/CVF Conference on Computer Vision and Pattern Recognition*, 2018, pp. 5020–5029.
- [27] Thuan D. Evolution of yolo algorithm and yolov5: the state-of-the-art object detection algorithm. 2021.
- [28] He K, Zhang X, Ren S, Sun J. Deep residual learning for image recognition. In *Proceedings of the IEEE conference on computer vision and pattern recognition*, 2016, pp. 770–778.
- [29] Lin T Y, Dollár P, Girshick R, He K, Hariharan B, Belongie S. Feature pyramid networks for object detection. In *Proceedings of the IEEE conference on computer vision and pattern recognition*, 2017, pp. 2117–2125.
- [30] Shrivastava A, Gupta A, Girshick R. Training region-based object detectors with online hard example mining. In *Proceedings of the IEEE conference on computer vision and pattern recognition*, 2016, pp. 761–769.
- [31] Shi B, Bai X, Yao C. An end-to-end trainable neural network for image-based sequence recognition and its application to scene text recognition. *IEEE transactions on pattern analysis and machine intelligence*, 2016, 39(11):2298–2304.
- [32] Krizhevsky A, Sutskever I, Hinton G E. Imagenet classification with deep convolutional neural networks. *Advances in neural information processing systems*, 2012, 25.
- [33] Redmon J, Divvala S, Girshick R, Farhadi A. You only look once: Unified, real-time object detection. In *Proceedings of the IEEE conference on computer vision and pattern recognition*, 2016, pp. 779–788.